JOURNAL OF APPLIED ELECTROCHEMISTRY 21 (1991) 945–960

REVIEWS OF APPLIED ELECTROCHEMISTRY 30

The continuous stirred tank electrochemical reactor. An overview of dynamic and steady state analysis for design and modelling

K. SCOTT

School of Science and Technology, Teesside Polytechnic, Middlesbrough, Cleveland TS1 3BA, Great Britain

Received 19 December 1990; revised 26 February 1991

The continuous stirred tank reactor is frequently adopted as a model for electrochemical reactors. This article brings together the various important aspects of the model: dynamics, thermal characteristics, residence time distributions and steady state characteristics and gives an overview of the design procedures.

Notation

A	magnitude of stepchange
C_j	concentration of species j (mol m^{-3})
C_f	friction factor
CE	current efficiency
C_j^s	concentration of species j at the surface (mol m^{-3})
C_{ji}	inlet concentration of species j (mol m^{-3})
C_p	heat capacity (J kg^{-1} K^{-1})
d_p	mean particle diameter (m)
D_e	dispersion coefficient
D_a	Damköhler number
e	voidage
E	electrode potential (V)
E_T	cell voltage (V)
E_d^0	decomposition potential (V)
f	parameter F/RT (V^{-1})
F	Faraday number
G_j	transfer function
H	enthalpy (kJ mol^{-1})
ΔH_r	heat of reaction (kJ mol^{-1})
ΔH_v	heat of vaporization (kJ mol^{-1})
i	current density (A m^{-2})
i_T	total current density (A m^{-2})
i^*	dimensionless current density $= i_1/n_1 F k_{LA} C_{A0}$
I	current (A)
I_j	partial current for reaction j (A m^{-2})
k	homogeneous reaction rate constant (s^{-1})
k_j	electrochemical rate constant in forward direction for step j (m s^{-1} (mol m^{-3})$^{1-w}$)
k_{-j}	electrochemical rate constant in reverse direction for step j (m s^{-1} (mol m^{-3})$^{1-w}$)
k_{bi}	reverse electrochemical rate parameter (m s^{-1})
k_{Lj}	mass transport coefficient of species j (m s^{-1})
K	equilibrium constant
K_p	gain
L	electrode length (m)
m	total mass of electrolyte (kg)
m_j	mass of components j (kg)
n	tank number
N	number of tanks
n_j	mol of species j
P	pressure (bar)
Q	heat flow (kJ s^{-1})
Q_{ex}	heat from external source (kJ s^{-1})
Q_v	enthalpy of vaporization (kJ s^{-1})
Q_L	heat losses (kJ s^{-1})
r_i	rate of electrode processes (mol m^{-3} s^{-1})
$r-i$	rate of electrode processes in reverse direction (mol m^{-3} s^{-1})
R	gas constant (kJ mol^{-1} K^{-1})
R_e	internal electrical resistance (Ω)
s	Laplace transform operator
S	surface area (m^2)
S	selectivity
t	time (s)
T	temperature (K)
T_i	inlet temperature of electrolyte (K)
u	velocity (m s^{-1})
U	overall heat transfer coefficient (kJ m^{-2} K^{-1} s^{-1})
v	volumetric flowrate of electrolyte
V	volume (m^3)
W	mean mass flowrate (kJ s^{-1})
w_1, w_2, w_j	reaction order exponents
x	dimension of reactor
X_1, X_2	perturbation variables
X_j	fractional conversion of species j
Y_1, Y_2	perturbation variables
z	dimensionless length
Bo	Bodenstein number
Pe	Peclet number
Re	Reynolds number
α'	transfer coefficient (V^{-1})

0021-891X/91 $03.00 + .12

β	coefficient defining potential dependence of electrochemical rate constant $= \alpha' nF$ (V^{-1})

Greek letters

$\bar{\eta}$	effectiveness factor
η	overpotential (V)
σ	specific surface area (m^{-1})
v	parameter $\sigma\tau$ ($s\,m^{-1}$)
ρ	density ($kg\,m^{-3}$)
τ	residence time (s)
τ_L	dimensionless residence time

Subscripts

a	anode
c	cathode
i	inlet

1. Introduction

The concept of the ideal continuous stirred tank reactor (CSTR) is well known in reaction engineering and is a familiar system for synthesis [1], albeit an ideal concept of fluid flow. The concept is applied successfully to the design of many reactors such as gas/liquid, liquid/liquid and fluidized bed systems. In principle, any fluid contacting region where some degree of mixing occurs can be approximated as either one well stirred region or a series of well stirred regions, through the concept of a non-idea flow model [2]. Furthermore when a reactor is operated with a low conversion per pass through the reaction region and a large proportion of the product stream is recycled back to the inlet, to achieve a high overall conversion, this also can be approximated as a CSTR. The flow characteristics of the reaction region itself do not have to be well mixed.

Recycle operation and multi-phase reactions are common in industrial electrolytic processes and the reactor model is well represented by the CSTR approximation. It has been adopted in a number of systems, such as the productions of sodium chlorate [3], the production of N-amino-2 methyl indoline [4], the epoxidation of ethylene [5] and the production of azoxytoluene [6]. The modelling of multiphase reactions, gas/liquid [7] and liquid/liquid [8], have also profited from the concept.

The CSTR has, not surprisingly, found use as an analytical device in rate modelling and kinetic analysis, (for example [9, 10]). The rudiments of the model have been presented by Pickett [11], whilst aspects of stability and thermal behaviour have been introduced by Fahidy [12].

This paper takes the opportunity to give an overview of the continuous stirred reactor as applied to electrochemical systems. Emphasis is on various aspects of the approach to modelling electrochemical reactors using the CSTR as a model. Steady state and dynamic analyses are presented for both isothermal and non-isothermal operations. The steady state models are geared towards providing the tools to predict product distributions, yields and current efficiencies and also the operating temperatures of the reactor.

The dynamic models are directed towards giving insight into how the reactor approaches the steady state, if indeed, it does and thus incorporating suitable "control" strategies. Linked with this aspect is the concept of non-ideal flow, which can be analysed from experimental tracer tests [1] based on the dynamic response of the reactor. In this respect a model of the reactor(s) is based on a cascade of well mixed flow regions and is referred to as the "tanks in series" model. By this means reactors which are intuitively not well mixed can be approached by the same design procedures as for a CSTR. In the limit of an infinite number of CSTR's, both the plug flow and batch reactor can be similarly analysed; a procedure which has been extensively used in numerical simulation.

Overall the concept of the CSTR is a powerful method in electrochemical reaction engineering for the analysis of single ideal reactors, multiple reactors and non-ideal reactors.

2. The continuous stirred tank reactor model

The ideal continuous stirred tank reactor is a device in which there is a complete mixing of the contents. It operates isothermally, with the composition and temperature of the exit solution matching the reactor contents.

When the CSTR reaches a steady-state condition it operates simultaneously in a constant current and constant voltage mode. Deviations from this are due solely to process dynamics, start-up and shut-down. The design procedures discussed make the reasonable assumption that the current density and electrode potential are uniform over the electrode surfaces. Also it is assumed that the mass transfer coefficients are independent of position and composition.

2.1. *The design equation*

The design equation for the CSTR operating at the steady state, comes directly from the material balance. It describes the concentration change over the reactor caused by reactions within. Referring now to Fig. 1, which depicts a unit of volume V. The flowrates into and out of the reactor are assumed equal and given by v and the inlet and outlet concentrations of species are C_{ji} and C_j, respectively.

For species A of reaction:

$$A + n_1 e^- \rightleftharpoons B \tag{1}$$

the material balance is

$$v(C_{Ai} - C_A) = \frac{i_1 S}{n_1 F} \tag{2}$$

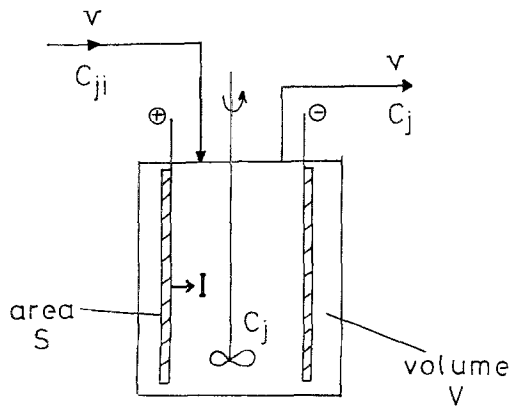

Fig. 1. Continuous stirred tank reactor model.

This equation can conveniently be written in terms of the residence time of fluid in the reactor, $\tau = V/v$, as

$$C_{Ai} - C_A = \frac{\sigma \tau i_l}{n_l F} \tag{3}$$

Electrochemical kinetics will be assumed to be described by Butler-Volmer type equations of the type

$$\frac{i}{nF} = k_{fl} C_A^S - k_{bl} C_B^S \tag{4}$$

with

$$k_{fl} = k_l \exp(-\alpha' nfE)$$

and

$$k_{bl} = k_{-l} \exp((1 - \alpha')nfE)$$

where $f = F/RT$ and C_A^S and C_B^S are surface concentrations and k_{fl} and k_{bl} are forward and reverse electrochemical rate constants, which can be written in a simplified form as

$$k_{fl} = k_l \exp(-\beta_l E)$$

$$k_{bl} = k_{-l} \exp((1 - \alpha')E)$$

β_l is essentially the slope of $\ln i$ against E, polarization data.

For a redox reaction, the design equation for component A, assuming first order reactions, is obtained as

$$C_{Ai} - C_A = \sigma\tau \frac{k_{fl} C_A - k_{bl} C_B}{(1 + D_{al} + D_{a2})} \tag{5}$$

where D_{al} and D_{a2} are modified Damköhler numbers defined as $D_{al} = k_{fl}/k_{LA}$ and $D_{a2} = k_{bl}/k_{LB}$.

An overall material balance on the reactor is written as

$$C_{Ai} = C_A + C_B \tag{6}$$

Eliminating C_B in Equations 5 and 6, with some rearrangement, gives

$$C_A = \frac{1 + \sigma\tau k_{bl}/(1 + D_{al} + D_{a2})}{1 + \sigma\tau(k_{bl} + k_{fl})/(1 + D_{al} + D_{a2})} \tag{7}$$

The fractional conversion is given by

$$X_A = \frac{\sigma\tau k_{fl}/(1 + D_{al} + D_{a2})}{(1 + \sigma\tau(k_{bl} + k_{fl})/(1 + D_{al} + D_{a2}))} \tag{8}$$

This expresses the performance of the CSTR in terms of the electrode potential, mass transport and reactor parameters σ and τ. The operating characteristics, are such that both galvanostatic and constant potential modes apply in operation. In other words neither current density nor electrode potential varies on any one electrode in the reactor. Changes in one of these two parameters are brought about by changing an operating variable such as τ, whilst holding the other parameter fixed. If one associated parameter is specified then the design is completed by estimating the remainder by virtue of the material balance and the rate.

For most practical situations electrochemical reactors will operate at high current densities and thus reaction will be of the irreversible (Tafel) type ($k_{bl} \to 0$). In this case Equation 8 truncates to

$$X_A = \frac{\sigma\tau k_{fl}}{(1 + D_{al} + \sigma\tau k_{fl})} \tag{9}$$

Equation 3 can be rewritten in terms of fractional conversion as

$$X_A = \left(\frac{\sigma\tau}{C_{Ai}}\right)\left(\frac{i_l}{n_l F}\right) = i^* \tau_L \tag{10}$$

where i^* and τ_L are the dimensionless current density and the residence time, respectively. Equation 10 can be used to determine the conversion as a function of operating current and feed rate (or current density and residence time).

From this the influence on performance of three important reactor parameters, i.e. specific electrode area, residence time and mass transfer coefficient is apparent. An increase in any of these will improve conversions, values of which are independent of reactant concentration. In practice it is not possible to adjust one of these parameters without affecting the other. For example, an increase in residence time can be brought about by reducing the flowrate, but the value of the mass transfer coefficient is usually dependent on flowrate and hence would be reduced. Additionally the reduction in flowrate may well cause a deviation from ideal mixing. Assessment of ideal mixing is considered later in this paper.

2.2. *Reactor cascades*

One of the major limitations of the continuous stirred tank reactor is that the reaction rate is controlled by the desired exit concentration of reactant from the system. Usually this concentration is low and hence so is the reaction rate. An approach to counteract this is to use a cascade of reactors in series (Fig. 2). Here the ideal mixing of the system is retained but because each tank except the last operates at a higher concentration, the overall rate of reaction is increased. Thus, for

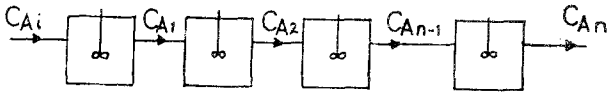

Fig. 2. Cascade of CSTR's.

equivalent conversions the cascade arrangement offers the opportunity of reducing total reactor size in comparison to a single unit.

Formulation of design procedures for reactor cascades requires, in principle, only the repetitive application of the design equations for individual units. Hence for each unit, n, in the cascade (7) is written in the form (for Tafel reactions).

$$\frac{C_{An}}{C_{An-1}} = \frac{1}{1 + \sigma\tau k_{f1}/(1 + D_{a1})} \tag{11}$$

Successive application of this over the reactor cascade gives

$$\frac{C_{An}}{C_{Ai}} = \frac{1}{\prod_{1}^{n}(1 + P_n)} \tag{12}$$

where $P = \sigma\tau k_{f1}/(1 + D_{a1})$ and the subscript, n, denotes its value for each reactor. If the reactors are of equal size and operate at identical electrode potentials, for example, to minimize side reactions, then Equation 12 reduces to

$$\frac{C_{An}}{C_{Ai}} = \left(1 + \frac{\sigma\tau k_{f1}}{(1 + D_{a1})}\right)^{-n} \tag{13}$$

Clearly this last expression has limiting forms for kinetic control and mass transport control of the reaction. The effect of a cascade arrangement on the size requirements of n equally sized reactors is shown in Fig. 3. Notice that although size requirements diminish when n increases, there is no direct proportionality. The benefits obtained in using a cascade arrangement in preference to a single larger unit must be balanced against the economics of the systems. A large number of small units may cost considerably more in terms of capital and running costs than a single unit.

Cascade arrangements of well-mixed reactors are likely to be encountered with rotating electrolysers for organic synthesis and metal recovery, fluidized beds and with gas/liquid reactions.

A final interesting point to note about the application of Equation 13 is the condition when $n \to \infty$, for which we obtain

$$\lim_{n\to\infty}\left(1 + \frac{\sigma\tau k_{f1}}{(1 + D_{a1})}\right)^{-n} = \exp\left(\frac{-\sigma\tau k_{f1}}{1 + D_{a1}}\right) \tag{14}$$

This, can be used as an approximate design equation for the plug flow reactor.

In treating general order reactions it is assumed that operation is at high current densities and kinetics are given by Tafel equations. The kinetic equation for Reaction 1 is written

$$\frac{i_1}{n_1 F} = k_{f1}(C_A^S)^{W_1} \tag{15}$$

where W_1 is the reaction order. When mass transport is not rate limiting Equation 15 is written in terms of fractional conversion, as

$$\frac{i_1}{n_1 F} = k_{f1} C_{Ai}^{W_1}(1 - X_A)^{W_1} \tag{16}$$

Application of Equation 16 is straightforward. The linear relationship between fractional conversion and current density, i.e. Equation 10, applies. Hence for any production rate the current is calculated and thus the electrode potential is found from Equation 16. Knowing this, the cell voltage is calculated from the general voltage balance.

The energy requirement for operation is constant at the steady state and is obtained simply from the product of the cell voltage, current and operating time.

The analysis of the CSTR requires solution of algebraic equations and if applied on the basis of constant current, is fairly simple. If a constant voltage or a constant electrode potential is applied, the analysis requires the solution of non-linear equations. In this case Equation 10 is combined with Equation 16 to give

$$X_A = \sigma\tau k_{f1} C_{Ai}^{(W_1 - 1)}(1 - X_A)^{W_1} \tag{17}$$

which relates the fractional conversion to the cell parameters σ and τ at a fixed electrode potential.

Solutions of this equation for reaction orders commonly found in electrosynthesis are given in Table 1.

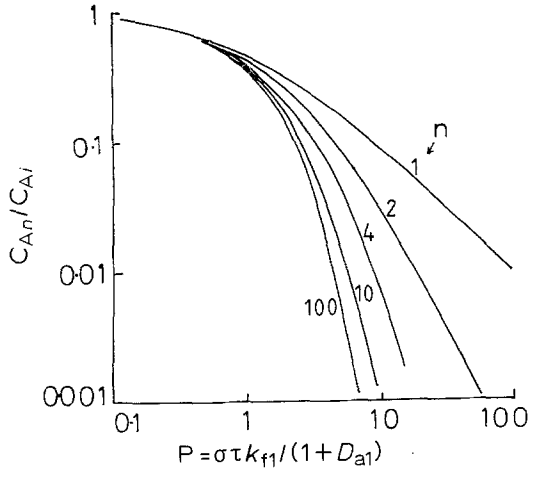

Fig. 3. Effect of reactor cascade on the size requirement.

Table 1. Fractional conversion in a CSTR for reactions of different order

Order W_1	*Conversion residence time relation,* X_A
0	$\sigma\tau k_{f1}/C_{Ai}$
$\frac{1}{2}$	$1 + \frac{\sigma\tau k_{f1}}{2(C_{Ai})^{1/2}} - \left(1 + \frac{(\sigma\tau k_{f1})^2}{4C_{Ai}}\right)^{1/2}$
1	$\frac{\sigma\tau k_{f1}}{1 + \sigma\tau k_{f1}}$
2	$1 - \frac{1}{2\sigma\tau\frac{1}{2}k_{f1}}\left\|((1 + 4k_{f1}\sigma\tau C_{Ai})^{1/2} - 1)\right\|$
−1	$\frac{1}{2}\left[1 - \left(1 - \frac{4\sigma\tau k_{f1}}{C_{Ai}^2}\right)^{1/2}\right]$

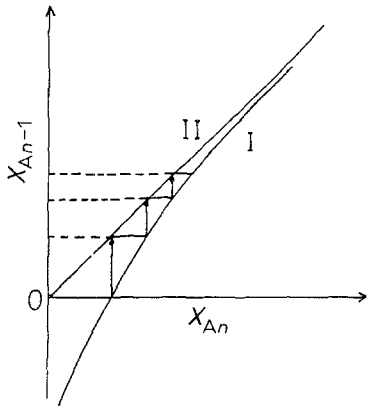

Fig. 4. Graphical Design method for reactor cascades.

With the reactor cascade numerical solutions of the coupled material balances will generally be required.

Alternatively a graphical design method, indicated by Eldridge and Piret [13] may be used. It is based on an equation of the form of Equation 10, in which the group $(\sigma\tau k_{f1})$ is preselected and independent of the number of reactors in the cascade.

The analysis of the problem is based on the material balance for a reactor in a cascade

$$C_{An-1} - C_{An} = \sigma\tau i_1/n_1 F \qquad (18)$$

which is now written in the form

$$X_{An-1} = X_{An} - \frac{\sigma\tau i_1}{C_{Ai} n_1 F} \qquad (19)$$

Thus X_{An-1} and X_{An} are uniquely related and can be presented graphically as shown in Fig. 4, as line I. When an auxillary line II, for which $X_{An-1} = X_{An}$, is also drawn, the horizontal distance from line I to line II is equal to $X_{An-1} - X_{An-1}$. A stepwise construction can thereby be made to estimate the number of reactors to achieve a desired conversion.

2.3. *Other considerations*

2.3.1. The effect of mass transport. Mass transport of species to and from an active surface is a physical process and its rate is essentially independent of the kinetic phenomena on the surface and is governed by the concentration driving force. An overall view of the physicochemical phenomena is that of a series of events, i.e. mass transport – electrode reaction – mass transport, providing there is no chemical reaction between reactants and products. If this is the case then the effect of simultaneous mass transport and chemical reaction may have an important bearing on the reaction pathway. This will be covered later.

The normal treatment of mass transport and reaction in series is based on the steady state principle; no accumulation of species at the surface. Hence the electrochemical reaction rate and the mass transport rate are equal and linked by the surface concentration. Thus for Reaction 1 the current density is given by

$$\frac{i_1}{n_1 F} = k_{f1} C_A^{sW_1} = k_{LA}[C_A - C_A^s] \qquad (20)$$

Table 2. Interphase effectiveness factors for general order kinetics

Reaction order W_1	*Effectiveness* $\bar{\eta}$
$n = \frac{1}{2}$	$\left[\frac{2 + D_{a0}^2}{2}\left(1 - \left[1 - \frac{4}{2 + D_{a0}^2}\right]^{1/2}\right)\right]^{1/2}$
$n = 2$	$\frac{1}{2D_{a0}}[(1 + 4D_{a0})^{1/2} - 1]$
$n = 1$	$\frac{1}{1 + D_{a0}}$
$n = -1$	$\frac{2}{1 + (1 - 4D_{a0})^{1/2}}$ $(D_{a0} \leqslant \frac{1}{4})$

From this expression, the relationship between current density and reactant concentration is

$$\frac{i_1}{n_1 F k_{LA}} + \left(\frac{i_1}{n_1 F k_{f1}}\right)^{1/W_1} = C_A, \quad (W_1 \neq 0) \qquad (21)$$

The fractional conversion, or reactant concentration, is related to the applied current at a given potential. The analysis can be completed from the known linear relationship (Equation 10) between i^* and X_A. Equation 21 will require numerical iteration for general reaction orders, although analytical expressions exist for reaction order of $\frac{1}{2}$, 2, -1 and, of course, 1. These equations can be conveniently expressed in terms of an interphase, or external, effectiveness factor, $\bar{\eta}$. This factor is the ratio of the global, or actual rate, to that of pure reaction or kinetic control.

Interphase effectiveness factors of a number of reaction orders are given in Table 2 as a function of a general (modified) Damköhler number

$$D_{a0} = \frac{k_{f1} C_{Ai}^{W_1 - 1}}{k_{LA}}$$

Figure 5 shows the functional variation of effectiveness with D_{a0}. The higher the order of reaction, the

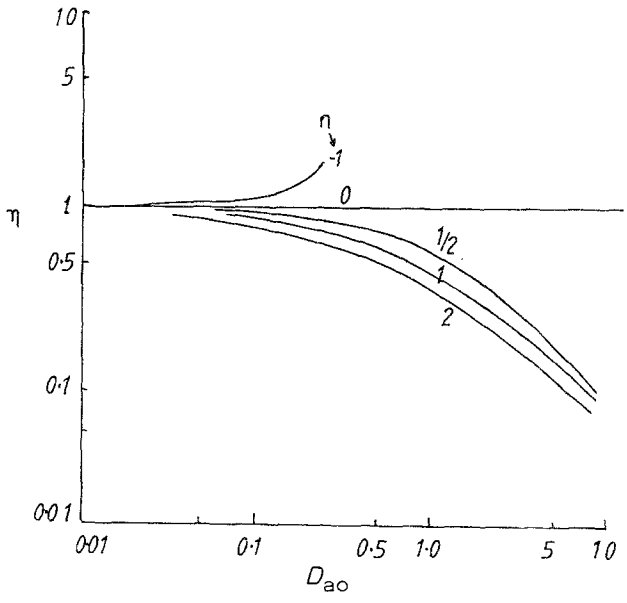

Fig. 5. Interphase effectiveness for general order reactions.

more telling the effect of mass transport limitations. For the negative reaction order, effectiveness actually increases, which is expected for reactions which are inhibited by high reactant concentrations. This is often induced by adsorption phenomena and is seen in the electrochemical oxidation of glucose to sorbital. In a similar way, zero order reactions are characterized by an effectiveness of unity.

2.3.2. Side reactions. The treatment of side reactions, which are independent of the main reaction, is straightforward for CSTR operation. For each reactant species (and product species) a material balance similar to Equation 10 is written. The rate of all ensuing reactions are coupled by the expression for total current density

$$i_T = \sum i_j \tag{22}$$

For a system of two reactions, $A = B$ and $C = D$, material balances for species A and C, combine with Equation 22 to give

$$\frac{i_T \sigma \tau}{F} = n_1 C_{Ai} X_A + n_3 C_{Ci} X_C \tag{23}$$

This describes the variation of fractional conversion of both species with the total current. The evaluation of conversions and current densities requires the simultaneous solution of Equation 23 and Equation 21 written for both reactions.

A goal with any set of independent reactions is to maximize the amount of desired product in relation to the amounts of by-products, i.e. the selectivity. For the CSTR only one selectivity is of interest, the steady-state ratio of the reaction rates.

$$S = \frac{(i_1/n_1F)}{(i_3/n_3F)} = \frac{(1 + D_{a3})k_{f1} C_A}{(1 + D_{a1})k_{f3} C_C} \tag{24}$$

Figure 6 shows some typical variations of selectivity with Damköhler number (D_{a1}).

Selectivity is favoured by high ratios of kinetic rate constants k_{f1}/k_{f3} and concentrations C_A/C_C. Two asymptotic cases are distinguishable:

(i) low Damköhler numbers, where mass transport controls and selectivity approaches the ratio C_A/C_C (when $k_{LA} = k_{LC}$)
(ii) high Damköhler numbers, where there is no mass transport limitation and the selectivity approaches the ratio of kinetic rate constants.

With reactions of general order the selectivity is given from Equations 15 and 24 as

$$S = \frac{k_{f1}(C_A^S)^{W_1}}{k_{f3}(C_C^S)^{W_3}} = \left(\frac{k_1}{k_3}\right) \exp\left((\beta_1 - \beta_3)E\right) \frac{(C_A^S)^{W_1}}{(C_C^S)^{W_3}} \tag{25}$$

Two factors which have great influence on the characteristics are electrode potential and reaction order. In the case of reaction order high selectivities are obtained by operating with high concentrations of A relative to C, when $W_1 > W_3$ and viceversa if $W_1 < W_3$.

The effect of electrode potential on selectivity is governed by the ratio of the coefficients β or Tafel slopes. If $\beta_1 < \beta_3$, then low potentials are favourable and if $\beta_1 > \beta_2$ then high potentials are favourable. Additionally the intrusion of mass transport limitations can have significant bearing on the choice of electrode potential.

2.4. *Multiple electrochemical reactions*

The CSTR with series reaction

As previously discussed, the operating characteristics of the ideal CSTR are such that constant potential, constant current and also constant voltage operation all apply. It will suffice to analyse the behaviour for Tafel type reactions for reaction sequence

$$A \xrightarrow{i_1} B \xrightarrow{i_2} C \tag{26}$$

The material balance for component B is written

$$C_B = \sigma\tau \left(\frac{i_1}{n_1F} - \frac{i_2}{n_2F}\right) \tag{27}$$

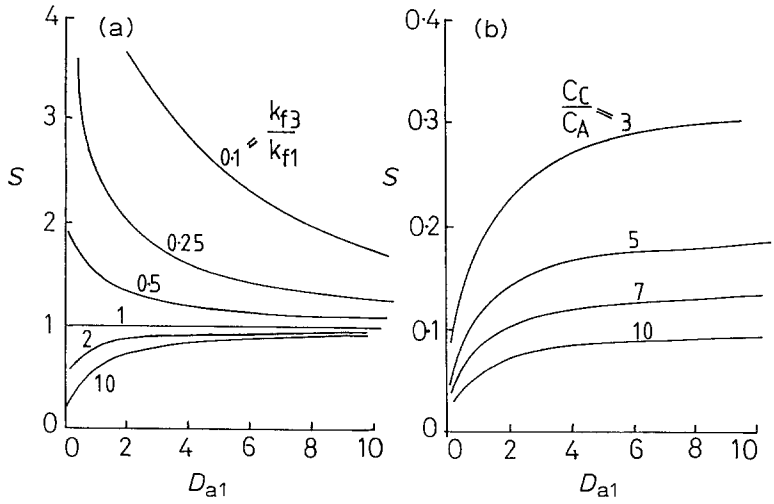

Fig. 6. Effect of Damköhler number on the selectivity of independent reactions. (a) $C_A/C_C = 1$ and (b) $k_{f1}/k_{f3} = 0.1$.

whilst the material balance on component A is

$$\frac{C_A}{C_{A0}} = \frac{1}{1 + \sigma\tau k_{f1}/(1 + D_{a1})} \quad (28)$$

The current density i_2 is written

$$\frac{i_2}{n_2 F} = \frac{k_{f1} D_{a1} C_A}{(1 + D_{a1})(1 + D_{a2})} + \frac{k_{f2} C_B}{(1 + D_{a2})} \quad (29)$$

Combining these equations the concentration of C_B is obtained as

$$\frac{C_B}{C_{A0}} = \frac{\sigma\tau k_{f1}}{(1 + D_{a1} + \sigma\tau k_{f1})(1 + D_{a2} + \sigma\tau k_{f2})} \quad (30)$$

The relationship between C_B/C_{A0} and conversion of C_B is obtained as

$$\frac{C_B}{C_{A0}} = \frac{X_A}{1 + D_{a2} + [(1 + D_{a1})X_A/k_{f1}(1 - X_A)]} \quad (31)$$

Series reactions, typically, exhibit a maximum (see Fig. 7) in intermediate concentration. This value is given by

$$\left(\frac{C_B}{C_{A0}}\right)_{max} = \left[(1 + D_{a2})\left(1 + \left[\frac{1 + D_{a1}k_{f2}}{1 + D_{a2}k_{f1}}\right]^{1/2}\right)^2\right]^{-1} \quad (32)$$

and is produced at a residence time given by

$$(\sigma\tau)_{max} = \left(\frac{(1 + D_{a1})(1 + D_{a2})}{k_{f1}k_{f2}}\right)^{1/2} \quad (33)$$

It can be seen from these expressions that poor rates of mass transport reduce the maximum concentration of B and increase $\sigma\tau$, at a fixed electrode potential. Typical yield-conversion characteristics for the CSTR are given in Fig. 7 and compared with equivalent performance for the batch (or PFR) reactor. The performance of the CSTR is inferior to that of the batch reactor. These characteristics apply to constant potential operation at fixed mass transport rates.

Changes in production specification will generally affect electrode potential and hence the ratio k_{f2}/k_{f1}. The total current density, i_T, will also change and is given by the following expression

$$\frac{\sigma i_T \tau}{C_{A0} F} = (n_1 + n_2)X_A - n_2(C_B/C_{A0}) \quad (34)$$

The performance of a CSTR is evaluated from Equations 28, 30 and 34. The influence of electrode potential depends on the relative values of Tafel slopes of both reactions. The greater the ratio of β_1/β_2 the higher the yield of B at the same electrode potential.

2.5. *Electrochemical reaction sequences involving chemical steps*

To illustrate the approach to the analysis of coupled electrochemical and chemical reactions, two reaction schemes are considered. The ECE mechanism, in which a chemical reaction is interposed between two electrochemical steps and an electrochemical reaction followed by competitive chemical and electrochemical steps. The analysis is restricted to first order reactions.

2.5.1. ECE reaction. For an ECE mechanism

$$A + n_1 e \xrightarrow{k_{f1}} I$$
$$I \xrightarrow{k_C} B \quad (35)$$
$$B + n_2 e \xrightarrow{k_{f2}} C$$

in which the intermediate I undergoes a slow pseudo first order reaction into an intermediate B, which can be further transformed by a second electron transfer to a stable product C.

For first order reaction, design equations for the CSTR configuration are

$$C_{A0} - C_A = \sigma\tau\,(C_A k_{f1}/(1 + D_{a1})) \quad (36)$$
$$C_I = \sigma\tau(C_A k_{f1}/(1 + D_{a1})) - \tau k_c C_I \quad (37)$$
$$C_B = \tau k_c C_I - \sigma\tau(C_B k_{f2}/(1 + D_{a2})) \quad (38)$$
$$C_C = \sigma\tau(C_B k_{f2}/(1 + D_{a2})) \quad (39)$$

where τ is the reactor holding time and k_C the chemical reaction rate constant for the second step in the reaction sequence.

Equation 8 describes the effect of system parameters on C_A. From Equations 8, 37 and 38 the yield of B, taken to be the desired product, is obtained as a function of conversion as

$$\frac{C_B}{C_{A0}} = \frac{\tau k_c \sigma\tau k_{f1} X_A}{(1 + \tau k_c))1 + D_{a1})(1 + \sigma\tau k_{f1})/(1 + D_{a2})} \quad (40)$$

The above expression can be modified to account for either EC or CE reaction mechanisms, by setting appropriate rate constants to zero. The influence of

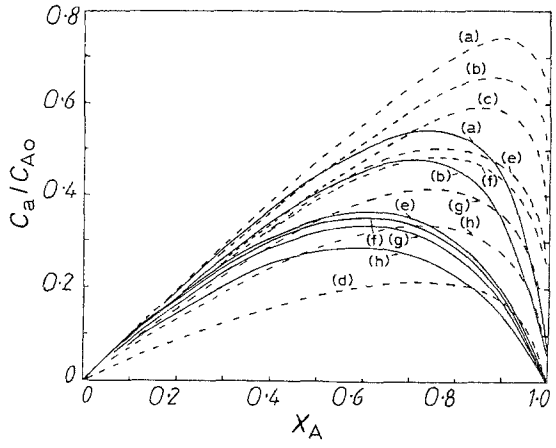

Fig. 7. Yield, conversion characteristics of series reaction. Solid lines (——): CSTR; dashed lines (– – –): plug flow.

Key	(a)	(b)	(c)	(d)	(e)	(f)	(g)	(h)
$\frac{k_{f1}}{k_{f2}}$	8.5	8.5	8.5	8.5	2.5	2.5	2.5	2.5
$\frac{k_L}{k_{f2}}$	170	17	8.5	0.85	25	12.5	5	2.5

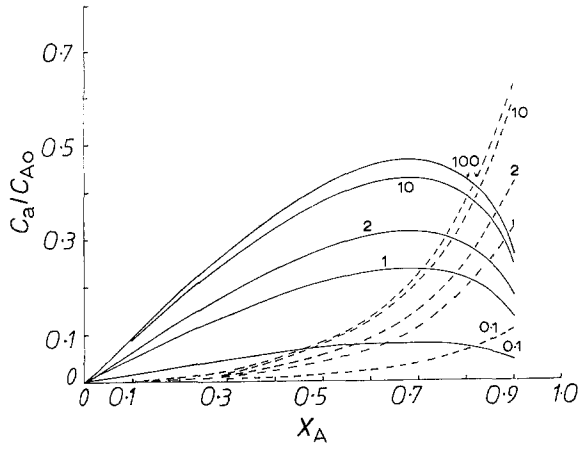

Fig. 8. Yield, conversion characteristics of an ECE reaction. Yield against conversion characteristics for series ECE reaction in a CSTR. $k_1 = 10^{-7}\,\mathrm{m\,s^{-1}}$, $k_2 = k_1/5$. $\beta_1 = \beta_2 = 20\,\mathrm{V^{-1}}$, $k_L = 3 \times 10^{-5}\,\mathrm{m\,s^{-1}}$. Solid lines (——): yield of B, C_B/C_{A0}; dashed lines (– – –): yield of C, C_C/C_{A0}. Values of $k\tau$ shown on figure.

simultaneous reactions such as solvent decomposition can be readily incorporated into the current balance.

Typical variations of yield versus conversion X_A, for this first order irreversible reaction sequence are given in Fig. 8 for the following operating conditions, $k_L = 3 \times 10^{-5}\,\mathrm{m\,s^{-1}}$, $k_1 = 10^{-7}\,\mathrm{m\,s^{-1}}$, $k_2 = k_1/5$, $\beta_1 = \beta_2 = 20\,\mathrm{V^{-1}}$. The effect of a variation in $k_c\tau$ is shown. The higher the value of $k_c\tau$, the greater the yield of intermediate product B (from the chemical reactions step). This product concentration goes through a maximum as conversion increases. After this maximum, the concentration of final product, C_C, rises rapidly. At low values of $k_c\tau$ (0.1), the levels of B and C produced are low, because the chemical step becomes effectively rate controlling.

These characteristics are typical of product distributions experienced with three step homogeneous reactions. As such the effect of variations in the orders of reaction of each step will also be analogous to the equivalent situation in homogeneous reaction analysis. This has already been seen for the series EE reaction. Where the series ECE system differ from the homogeneous counterpart is in the influence of electrode potential on the electrochemical parameter. As with the series EE scheme, the ratio of Tafel slopes will significantly influence yields of intermediate. Conditions generally favourable to high yields of B are a high value of the ratio $k_{f1}/\tau k_c$ and a low ratio of $k_{f2}/\tau k_c$.

Typical variations of the yields of intermediate B and conversion of A with electrode potential are given in Fig. 9 for reactions not limited by mass transport. The anticipated influence of Tafel slopes on performance is shown, that is the higher the ratio of β_1/β_2, the greater the yield of B.

The effect of mass transport on performance is also shown in Fig. 9. When $\beta_1 > \beta_2$, lower mass transport rates depress the maximum yield of B. At high potentials, yields of B reach limiting values, due to the onset of limiting current characteristics (and the use of constant v). When $\beta_1 < \beta_2$, the effect of slow mass transport can be such that the occurrence of a maximum yield of B is eliminated.

2.5.2. Competing electrochemical/chemical reactions. For the mechanism

$$\left.\begin{aligned} A + n_1 &\longrightarrow B \\ B &\xrightarrow{k_c} R \\ B + n_2 e &\longrightarrow C \end{aligned}\right\} \qquad (41)$$

where the intermediate B can either undergo pseudo first order irreversible homogeneous transformation into a stable product R or further heterogeneuos electrochemical transformation to the stable product C. Again restricting the analysis to first order electrochemical reaction, CSTR design equations for species B, R and C are

$$C_B = \left(\frac{\sigma\tau k_{f2}}{1 + D_{a2}}\right)\left(\frac{C_A k_{f1}}{k_{f2}(1 + D_{a1})} - C_B\right) - \tau k_c C_B \qquad (42)$$

$$C_R = \tau k_c C_B \qquad (43)$$

$$C_C = \sigma\tau(C_B k_{f2}/(1 + D_{a2})) \qquad (44)$$

The total current density is given by

$$i_T = \frac{k_{f2} C_B}{1 + D_{a2}} + \frac{k_{f1} C_A}{(1 + D_{a1})}\left(1 + \frac{1}{(k_{f2} + k_{LB})}\right) \qquad (45)$$

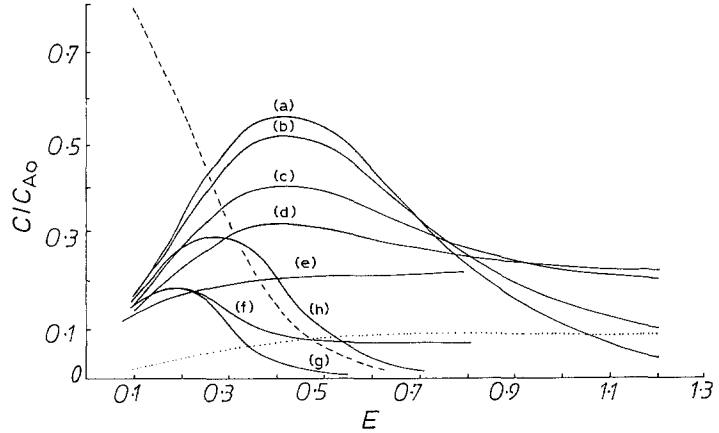

Fig. 9. Effect of electrode potential on intermediate product yield in a CSTR. Variation of intermediate product yield with electrode potential for a ECE reaction. $vk_1 = 10^{-1}$, $\beta_1 = 10\,\mathrm{V^{-1}}$, $k_0\tau = 10$, $k_2/k_1 = 0.5$.

Key	(a)	(b)	(c)	(d)	(e)	(f)	(g)	(h)
$\beta_2(\mathrm{V^{-1}})$	5	5	5	5	15	15	15	10
$\frac{k_1}{k_L}$	0	0.01	0.05	0.1	0.1	0.01	0	0

Dashed lines (– – –): C_A/C_{A0} for $k_L \to \infty$ and $\beta_2 = 5$; dotted lines (· · · ·): C_I/C_{A0} for $k_L \to \infty$ and $\beta_2 = 5$.

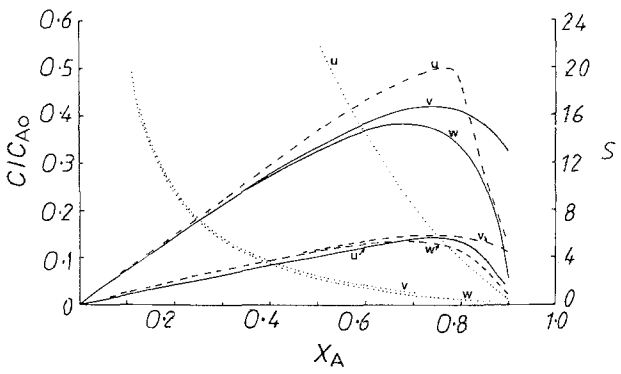

Fig. 10. Performance characteristics of a series, parallel electrochemical reaction. Solid lines (——): C_B/C_{A0}; dashed lines (– – –): C_R/C_{A0}; dotted lines (· · · ·): selectivity S.

Key	(u)	(v)	(w)
τ (s)	10^4	10^3	10^3
k_L (ms^{-1})	10^{-5}	10^{-4}	10^{-5}

Usually either R or C will be desired product in this reaction scheme and the selectivity of say, R, is given by

$$\frac{C_R}{C_C} = \frac{k_c(1 + D_{a2})}{\sigma k_{f1}} \tag{46}$$

Thus electrode potential and mass transfer coefficient will tend to govern selectivity. These design equations and those in previous sections will be used to illustrate typical performance characterstics of the CSTR.

Reactions schemes which consist of both simultaneous and series steps can often pose problems in the selection of flow characteristics for effective operation. Generally for isopotential systems mixing favours the production of ultimate products for series reactions, because the yield of intermediate is lower. For parallel reaction mixing favours the reaction of lowest order. If both steps are of equal order, then flow characteristics do not influence selectivity.

A reaction sequence typical of this competing electrochemical and chemical scheme is the reduction of nitrobenzene (A) to the intermediate phenylhydroxylamine (B). Phenylhyroxylamine (B) then either undergoes chemical rearrangement to p-aminopheol

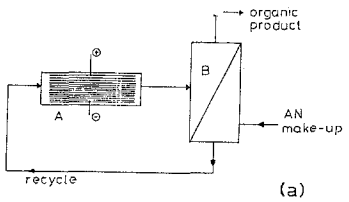

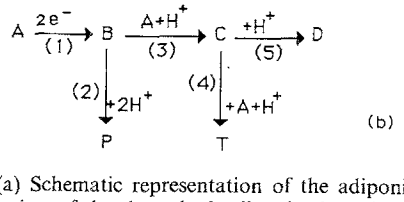

Fig. 11. (a) Schematic representation of the adiponitrile reactor; (b) mechanism of the electrohydrodimerization of acrylonitrile.

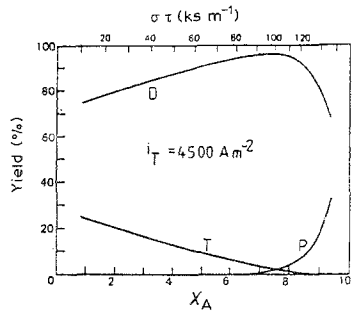

Fig. 12. Product distributions for the synthesis of adiponitrile.

(R) or is reduced electrolytically to aniline (C). A recent analysis [14] of this reaction scheme has indicated the following kinetics, for electrolysis is highly acidified aqueous, organic media

$$k_{f1} = 1.2 \times 10^{-7} \exp\left(\frac{-2.3E}{0.17}\right) \text{m s}^{-1}$$

$$k_{f2} = 1.7 \times 10^{-8} \exp\left(\frac{-2.3E}{0.17}\right) \text{m s}^{-1}$$

$$k_c = 3.5 \times 10^{-4} \text{ s}^{-1}$$

This data is used to predict typical CSTR performance characteristics shown in Fig. 10 for a value of $v = 10^6 \text{ s m}^{-1}$.

Typical variations of the concentration of B and R and selectivity S, with fractional conversion are shown. The intermediate B, as expected, goes through a maximum value. The selectivity S decreases from high initial values at low conversions (due to relatively low operating potentials and current densities), to very low values at high conversions. Here chemical reaction is slow in comparison to the competitive electrochemical step to C, due to the high potentials of operation. This behaviour is reflected in the variation in concentration of R, which goes through a maximum.

The effect of an increase in mass transport is shown in Fig. 10, to increase the concentrations of both B and R, especially at high conversion and also the selectivity. The effect of a variation in reactor holding time is also seen in Fig. 10. Overall, at higher τ, C_B is lower and C_R and selectivity S are both higher.

From operating characteristics just described above it can be appreciated that the need to achieve good yields with good selectivity, must be balanced against the production limitations of high reactor holding time and cost restrictions of reactor size, high mass transport and cell currents i.e. power consumption and current efficiency.

2.6. *An industrial synthesis — The production of adiponitrile*

The electrohydrodimerization of acrylonitrile to adiponitrile is a major industrial electro-organic synthesis. The reactor unit used is shown schematically in Fig. 11. The reactor electrode banks are continuously supplied with aqueous electrolyte containing acrylonitrile recycled from the separator. Organic product is produced as a second phase which, is decanted off the

aqueous phase in a separator. The organic product is then processed downstream to produce crude adiponitrile product and a recycle acrylonitrile stream. The reaction yields two major by-products, propionitrile (P) and a trimer (T), as well as adiponitrile (D). A mechanism which satisfies the chemistry associated with adiponitrile formation, involves the electrochemical reduction to a dianion derivative (B) prior to a sequence of chemical reactions. The overall mechanism is shown in Fig. 11.

In the sequence of reactions intermediates B and C are formed in small quantities. The application of the stationary state approximation to these species ($dC_j/dt = 0$) simplifies the analysis through the resultant equalities

$$C_B^S = \frac{k_1 C_A^S}{k_2 + k_3 C_A^S}; \qquad C_C^S = \frac{k_3 C_A^S C_B^S}{(k_5 + k_4 C_A^S)} \tag{47}$$

The mass transport of A to the electrode is described by

$$k_L(C_A - C_A^S) = \frac{i_1}{n_1 F} + k_3 C_A^S C_B^S + k_4 C_A^S C_C^S \tag{48}$$

The material balances for this unit approximated as a CSTR in which organic product is formed as the second dispersed phase can be written as

$$C_{A0} = C_A + \sigma\tau\left[\frac{i_T - i_S}{nF} + k_3 C_A^S C_D^S + k_4 C_A^S C_C^S\right] \tag{49a}$$

$$\left.\begin{aligned} C_P &= \sigma\tau k_2 C_B^S \\ C_D &= \sigma\tau k_5 C_C^S \\ C_T &= \sigma\tau k_4 C_A^S C_C^S \end{aligned}\right\} \tag{49b}$$

In these the term i_s refers to the current density associated with hydrogen evolution and oxygen reduction.

Combining Equations 48 and 49 enables the surface concentration of A to be obtained as

$$C_A^S = C_A\left(1 + \frac{1}{k_L\sigma\tau}\right) - \frac{C_{A0}}{k_L\sigma\tau} - \frac{i_s}{nFk_L} \tag{50}$$

As an approximation the current density, i_s, can be considered constant, i.e. oxygen reduction is at its limiting current and electrode potential variations have only a small influence on hydrogen evolution.

The solution to the reactor model is achieved by solving Equations 47 and 48 (which give a cubic equation in C_A^S) simultaneously at fixed values of mass transport and reactor parameters. The value of C_A^S is then substituted into Equations 49a and b to give the product distribution.

The variation of product distribution obtained from this procedure are shown in Fig. 12.

The yield of adiponitrile goes through a maximum with increasing conversion, caused by increasing the value of current density or reactor parameter $\sigma\tau$. With increasing conversion, the yield of propionitrile increases whilst that of trimer decreases. Acrylonitrile concentration is particularly crucial in obtaining high adiponitrile yields although at the conditions for maximum yield, both propionitrile and trimer are formed in significant quantities.

Generally the yields obtained from this model are in agreement with the performance of the adiponitrile synthesis reactor.

3. Dynamics and Non-Ideal Flow

3.1. *Non-ideal flow*

The dynamic model of the CSTR gives a convenient means for the analysis of non-idea flows in electrolytic reactor which are conceptually treated as having plug flow or well mixed characteristics. This is referred to as the tanks in series model and is one of two widely used single parameter models for non-ideal flow; the other being the dispersed plug flow model [1]. An advantage of the tanks in series model is that with cascades of reactors or well mixed flow regions, non ideality in flow in each region merely increases the effective number of reactors in the overall cascade.

3.2. *The tanks in series model*

This widely used single parameter model visualizes the flow as passing through a series of n well-mixed regions. The model is therefore similar to that used to analyse the cascade arrangement of equal sized CSTR's where the number of tanks, N, is determined from residence time distribution data. This is done by considering the dynamics of a series of N tanks to say, a tracer impulse [2].

The C-diagram (concentration-time diagram) for a series of N tanks shown in Fig. 13 is determined for the

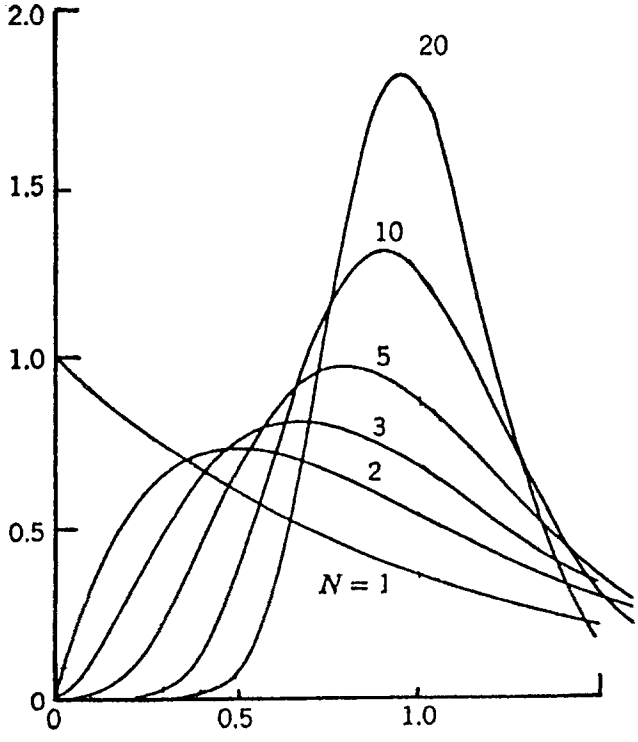

Fig. 13. The tanks in series model and the dynamic response to a tracer impulse.

material balances written generally for the nth tank as

$$\frac{V\mathrm{d}C_n}{\mathrm{d}t} = v(C_{n-1} - C_n) \tag{51}$$

where V is the volume of one well-mixed region. Introducing the following dimensionless notation

$$\theta = \frac{t}{\tau}, \quad \tau = \frac{NV}{v}, \quad C_n = \frac{C_n}{C_0}$$

where C_0 is the concentration of tracer introduced into the series of tanks. In this, τ is the mean residence time for the N tank system.

The material balance becomes

$$\frac{1}{N}\frac{\mathrm{d}C}{\mathrm{d}\theta} = C_{n-1} - C_n \tag{52}$$

Solving this, using Laplace transforms, gives

$$\frac{-C_n(o)}{N} + s\frac{C_n}{N} = C_{n-1} - C_n \tag{53}$$

With $C_n(o) = 0$, this rearranges to

$$\frac{C_n}{C_{n-1}} = \frac{1}{1 + s/N} \tag{54}$$

For the nth tank this can be written as

$$\frac{C_n}{C_1} = \left(\frac{1}{1 + s/n}\right)^n \tag{55}$$

with $C_1 = 1$. Reverse transformation of Equation 55 gives

$$C_{n(\theta)} = \frac{N(N\theta)^{n-1}\exp(-N\theta)}{(n-1)!} \tag{56}$$

The characteristics of this C-curve are shown in Fig. 13. Similarities with the dispersion model are evident [2], especially with a relatively large number of tanks. Typical values of N for a parallel plate electrolytic reactor are shown in Fig. 14, versus Reynolds number, based on the hydraulic mean diameter of the channel D_{Hm}. This is estimated from previously published data [2] based on the correlation of the Bodenstein number, $Bo = uD_{\mathrm{Hm}}/D_e$, with friction factor, C_f, for cylindrical pipes

$$Bo = 0.28/C_f^{1/2} \tag{57}$$

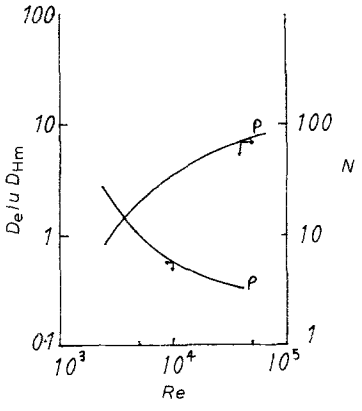

Fig. 14. Variation of Peclet number and N in a parallel plate reactor.

One of the advantages of the tanks in series model over the dispersion model is in its application with multiple reactions, in that it requires only the solution of the simultaneous algebraic equations. The dispersion model requires the solution of differential equations, which can only be achieved analytically for first order (and zero order) reactions operating at a constant electrode potential and then solutions are cumbersome. The tanks in series model requires only the repetitive calculations of the design equations presented in § 2.4.

3.2. *Dyamics of the isothermal CSTR*

The dynamics of CSTR's are important due to considerations of stability, control and operating procedures. Two approaches to modelling are generally considered, analytical models of linear or linearized systems and dynamic simulation based on numerical methods. Both these aspects are considered briefly here in the context of electrochemical reactions.

3.2.1. Analytical models. The dynamic behaviour of a single isothermal CSTR is obtained from the material balance

$$V\frac{\mathrm{d}C_{A2}}{\mathrm{d}t} = v(C_{A1} - C_{A2}) - \frac{\sigma iV}{nF} \tag{58}$$

Identifying the perturbation variables, $Y = C_{A2} - C_{A2}^+, X_1 = C_{A1} - C_{A1}^+, x_2 = i - i^+$, where the superscript $(^+)$ denotes the corresponding steady-state value, Equation 58 can be written as

$$\frac{\mathrm{d}Y}{\mathrm{d}t} + \frac{Y}{\tau} = \frac{X_1}{\tau} - \frac{\sigma X_2}{nF} \tag{59}$$

Introducing Laplace transforms and re-arranging this

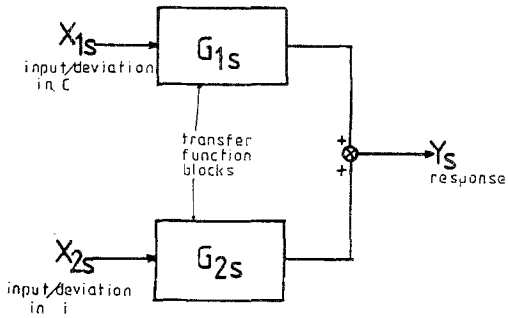

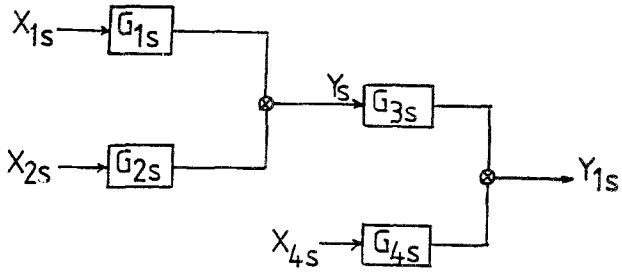

Fig. 15. Block diagram for CSTR dynamic model.

becomes

$$Y_s = \frac{X_{1s}}{\tau s + 1} - \frac{X_{2s}\sigma\tau/nF}{\tau s + 1} \quad (60)$$

This equation represents an input–output model of the reactor, describing the dynamic behaviour. The terms $1/(\tau s + 1) = (G_1)_s$ and $(\sigma\tau/nF)/(\tau s + 1) = (G_2)_s$ are the transfer functions of the process. The system can be represented as a block diagram, as shown in Fig. 15.

To illustrate the application consider the response of the reactor to step changes in input variables.

In the absence of a perturbation in current, consider the effect of a step change in X_1. The Laplace transform of a step change of magnitude A is A/s. Therefore Equation 59 becomes

$$Y_s = \frac{A}{s(\tau s + 1)} \equiv \frac{A}{s} - \frac{A\tau}{(\tau s + 1)} \quad (61)$$

Inverting Equation 61 gives

$$Y = A(1 - \exp(-t/\tau)) \quad (62)$$

This is the response of a "first order lag" of transfer function $(G_1)_s$ which as $t \to \infty$, $Y \to A$, the new inlet variable (concentration).

If the system is now subjected to only a perturbation in current density ($X_{1s} = 0$), say a step of magnitude A, then the response is

$$Y = -A\frac{\sigma\tau}{nF}(1 - \exp(-t/\tau)) \quad (63)$$

Again as $t \to \infty$ the system approaches a steady-state concentration given by $A\sigma\tau/F$. In this system the group $-\sigma\tau/nF$ is referred to as the steady-state "gain", K_p, of the process since for any change in input, Δ_i, the change in output Δ_O is given by $\Delta_O = K_p\Delta_i$. If perturbations in both feed concentration and current density occur then the response is the sum of Equations 62 and 63.

For a cascade of tanks the transfer function is composed of the transfer functions of the individual elements in the system. For example a cascade of two tanks the transformed equation in terms of perturbation variables is

$$Y_{1s} = \frac{Y_s}{\tau_1 s + 1} - \frac{\sigma_1 X_{4s}\tau_1/nF}{\tau_1 s + 1} \quad (64)$$

where τ_1 is the residence time of the second tank and X_{4s} represents the perturbation variable for the current density in the second tank. Combining Equations 60 and 63 the transformed equation representing this system is

$$Y_{1s} = \frac{X_{1s}}{(\tau s + 1)(\tau s + 1)} - \frac{\sigma\tau/nF)X_{2s}}{(\tau s + 1)(\tau_1 s + 1)} - \frac{(\sigma_1\tau_1/nF)X_{4s}}{(\tau_1 s + 1)} \quad (65)$$

and is shown in block notation in Fig. 15.

The response of the system to a step change in inlet concentration is from Equation 65

$$Y = A \times \left[1 - \frac{1}{(\tau_1 - \tau)}(\tau\exp(-t/\tau) - \tau_1\exp(-t/\tau_1))\right] \quad (66)$$

The system response is sluggish as the time to reach a new steady state for the second tank suffers from a "transfer lag". In a similar way any perturbation in current in the first tank will be slower to affect the concentration change in the second tank.

In the above the current supplied to the reactor is independent of conditions in the reactor. If an approximate potentiostatic operation exists then the material balance for one tank can be written as

$$\tau\frac{dC_{A2}}{dt} + C_{A2} = C_{A1} - \sigma\tau k' C_{A2} \quad (67)$$

where $k' = k_{f1}/(1 + D_{a1})$. In terms of perturbation variables this becomes

$$Y_s = \frac{X_{1s}}{(\tau s + 1 + \sigma\tau k')} \quad (68)$$

With a step change in concentration of magnitude A this gives, on inversion

$$Y = \left(\frac{A}{1 + \sigma\tau k'}\right)(1 - \exp[-(t/\tau)(1 + \sigma\tau k')]) \quad (69)$$

The gain of this system is $1/(1 + \sigma\tau k')$. The transfer function for a cascade of CSTR's follows from Equation 68, knowing the relationship for "non-interacting" systems.

For a two tank system the model is of a form similar to Equation 67 where τ_1 and τ are replaced by $\tau_1/(1 + \sigma_1\tau_1 k_1')$ and $\tau/(1 + \sigma\tau k)$, respectively, and A by $A/(1 + \sigma\tau k')(1 + \sigma_1\tau_1 k_1')$.

If operating conditions of both tanks are identical then the following equation applies

$$Y = \frac{A}{(1 + \sigma\tau k')^2} \times \left[1 - \left(\frac{\tau/(1 + \sigma\tau k') + t}{\tau/(1 + \sigma\tau k')}\right)\exp[-(t/\tau)(1 + \sigma\tau k')]\right] \quad (70)$$

Typical response curves for this system for a unit step change in concentration are shown in Fig. 16. The selection of a perturbation in concentration is quite arbitrary. Perturbations in flowrate and electrode potential may also arise. To develop transfer functions for this system the dynamic material balance must be written in an approximate linear form [12].

3.2.2. Dynamic response from analytical solution for multiple reaction. To illustrate the analysis for complex reactions consider the consecutive sequence $A \to B \to C$, in which the effective electrochemical

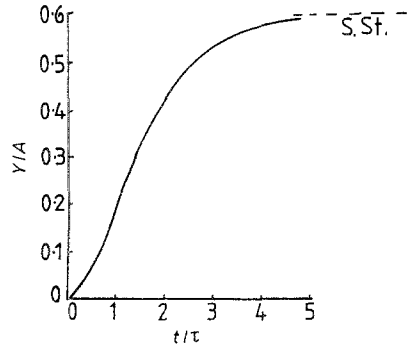

Fig. 16. Response of a cascade of two CSTR's.

rate parameters for successive steps are k_1' and k_2'. For a CSTR the dynamic model is expressed in terms of the following perturbation variables,

$$Y_1 = C_{A2} - C_{A2}^+, \quad X_1 = C_{A1} - C_{A1}^+$$

and

$$Y_2 = C_{B2} - C_{B2}^+$$

For potentiostatic control,

$$\frac{dY_1}{dt} + \frac{Y_1}{\tau} = \frac{X_1}{\tau} - \sigma k' Y_1 \tag{71}$$

$$\frac{dY_2}{dt} + \frac{Y_2}{\tau} = \sigma k_1' Y_1 - \sigma k_2' Y_2 \tag{72}$$

The response is obtained by the solution of the coupled equations using Laplace transforms.

For a step change in inlet concentration, $X_{1s} = A/s$, the solution of equation in the form of Equation 70 while for Equation 72 it is obtained from

$$Y_{2s} = \frac{\tau\sigma k_1' A}{s(\tau s + 1 + \sigma\tau k_2')(\tau s + 1 + \sigma\tau k_1')} \tag{73}$$

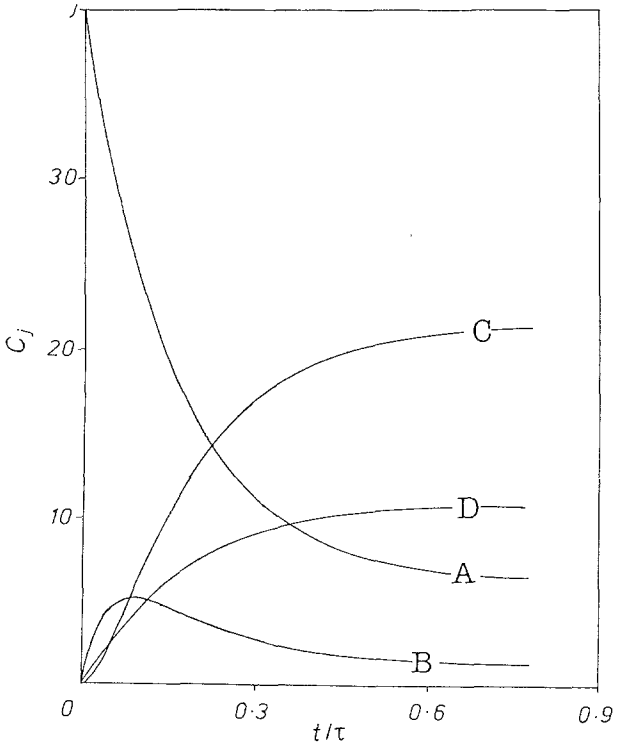

Fig. 17. Dynamic response of a CSTR for p-amino phenol production, $\tau = 10^5$ s, $E = -0.35$ V.

The response of the concentration of B to a step change in concentration of A is thus obtained from the transfer function of an "overdamped" second order system. The solution of this is

$$Y_{2s} = (\sigma k_1' A/\tau)[C + A \exp(-p_1 t) + B \exp(-p_2 t)] \tag{74}$$

where $p_1 = (1 + \sigma\tau k_2')/\tau$, $p_2 = (1 + \sigma\tau k_2')/\tau$, $C = 1/p_1 p_2$, $A = -1/p_1(p_2 - p_1)$ and $B = 1/p_2(p_2 - p_1)$. This expression exhibits a characteristic exponential approach to steady state, expected of the two first order lags of Equation 73. The greater the values of rate parameters the faster the system approaches a new steady state. Equation 74 is also applicable to the start-up of a reactor assuming the system electrode potential is initially zero and rapidly stepped to its operating value.

3.2.3. Dynamic response from dynamic simulation. The Laplace transform technique is limited because of the restriction of linearity of the differential equation. General order reactions usually cannot be analysed nor can modes of operation other than constant potential. Dynamic simulation of the reactor will frequently be required for multiple reactions. Such a technique has been used for the simulation of the dynamic response of a potentiostatically controlled CSTR for *p*-amino phenol production. This chemical is formed by the reaction mechanism described in §2.5.2.

The typical response of this system is shown in Fig. 17 where under the conditions employed, steady state is approached at a time approximately equal to the residence time. The response curves reflect the nature of the reaction pathway, i.e. the intermediate B exhibits a maximum. From dynamic simulation of a CSTR we see that the response curves resemble those obtained with a batch reactor.

4. Analysis of the thermal behaviour of a CSTR

Operating temperature can play a crucial role in electrochemical cell and reactor performance. From a thermal balance of a cell, the dynamic and steady state behaviour can be determined, thus enabling the specifications of conditions and parameters. For desired operation, a thermal energy balance for a CSTR can be formulated

$$Q_A = Q_E - Q_{HL} + Q_{ex} \tag{75}$$

where the terms Q refer to thermal energy accumulated, generated by electrolysis, heat losses and heat from external sources, respectively.

The thermal energy generated by electrolysis is given by

$$Q_E = I(E_T - \Delta H_r/nF) \tag{76}$$

The heat losses are the sum of that due to external heat exchange that due to vaporization of electrolyte and that due to enthalpy change of flowing liqid through

the cell, i.e.

$$Q_{HL} = Q_L + Q_F + Q_V$$
$$= \sum UA(T_s - T_a) + \sum W_i C_{pi}(T_d - T_i)_{\text{product-reactant}} + W_V \Delta H_V \quad (77)$$

Considering the reactor to be a single compartment CSTR in which the temperature of the electrolyte is everywhere uniform and equal to the exit temperature. Assuming the mass flowrate of electrolyte through the cell to be constant, i.e. W and also that the mass, m, of electrolyte in the cell remains constant, the thermal energy balance can be written as

$$m\bar{C}_p \frac{dT_s}{dt} = I\left[E_T - \frac{\Delta H_r}{nF}\right] + \bar{W}\bar{C}_p(T_i - T_s) - Q_L - Q_v + Q_{ex} \quad (78)$$

The steady state temperature is thus obtained from

$$IE_T = \left(\frac{I\Delta H_r}{nF}\right) + \bar{W}\bar{C}_p(T_5 - T_i) + Q_L + Q_v - Q_{ex} \quad (79)$$

where $\bar{C}_p$ is a mean heat capacity for all components in the electrolyte.

Integration of Equation 78 enables the dynamics of the CSTR to be determined. In general this can be an involved procedure requiring simultaneous solution with appropriate material balances. However a good approximation, at least when only electrochemical reactions are involved is to consider chemical changes in the system to be insignificant. The physical properties of the electrolyte, C_p, E_T, ΔH_r and ΔH_v in general vary with temperature. A first order representation of this variation, valid over a moderate temperature range, is through linear regression. Thus the physical properties can be represented by:

Heat of vaporization

$$\Delta H_v = a_1 + b_1 T \quad (80)$$

Electrolyte conductivity

$$K = a_2 + b_2 T \quad (81)$$

Enthalpic voltage (or enthalpy of reaction)

$$\Delta H_r = a_3 + b_3 T \quad (82)$$

Decomposition voltage

$$E_d^0 = a_4 + b_4 T \quad (83)$$

The unsteady-state thermal energy balance for a constant current and constant evaporation rate becomes

$$m\bar{C}_p \frac{dT_s}{dt} = I\left[\Sigma|\eta| + a_4 + b_4 T_s + \frac{Id}{S(a_2 + b_2 T)} - (a_3 + b_3 T_s)\right] + \bar{W}\bar{C}_p(T_i - T_s) - \Sigma UA(T_s - T_a - \bar{W}_v(a_1 + b_1 T_s) \quad (84)$$

Defining the following lumped parameters

$$\gamma_1 = b_2(b_4 I - b_3 I - \Sigma UA - \bar{W}_v b_1 + \bar{W}\bar{C}_p) \quad (85)$$

$$\gamma_2 = \frac{a_2\gamma_1}{b_2} + b_2[I\Sigma|\eta| + a_4 I - a_3 I + \Sigma UAT_a + \bar{W}\bar{C}_p T_i] \quad (86)$$

$$\gamma_3 = a_2(I\Sigma|\eta| + a_4 I - a_3 I + \Sigma UAT_a - \bar{W}_v a_1 + \bar{W}\bar{C}_p T_i) + I^2 d/S \quad (87)$$

Equation 84 becomes

$$t = \int_{T_i}^{T_s} \left(\frac{m\bar{C}_p(a_2 + b_2 T_s)}{\gamma_1 T_s^2 + \gamma_2 T_s + \gamma_3}\right) dT_s \quad (88)$$

On integration this gives

$$t = \frac{m\bar{C}_p b_2}{2\gamma_1} \ln\left[\frac{\gamma_1 T_s^2 + \gamma_2 T_s + \gamma_3}{\gamma_1 T_i^2 + \gamma_2 T_i + \gamma_3}\right] - \int_{T_i}^{T_s} \left(\frac{mC_p b_2\gamma_2/2\gamma_1 - mC_p a_2}{\gamma_1 T_s^2 + \gamma_2 T_s + \gamma_3}\right) \quad (89)$$

The integration of the second term in this equation depends on the roots of the quadratic in the denominator. For a typical criterion of $\gamma_2^2 < 4\gamma_3$, the final equation becomes

$$t = \frac{m\bar{C}_p b_2}{2\gamma_1} \ln\left[\frac{\gamma_1 T_s^2 + \gamma_2 T + \gamma_3}{\gamma_1 T_i^2 + \gamma_2 T + \gamma_3}\right] - \left(\frac{m\bar{C}_p b\gamma_2}{2\gamma_1} - m\bar{C}_p a_2 \frac{1}{\beta}\right) \times \left[\tan^{-1}\left(\frac{T_s - \alpha}{\beta}\right) - \tan^{-1}\left(\frac{T_i - \alpha}{\beta}\right)\right] \quad (90)$$

where $\{\alpha \text{ and } \beta\} = \frac{1}{2}\{(-\gamma_2/\gamma_1) \pm [(\gamma_2/\gamma_1)^2 - 4(\gamma_3/\gamma_1)]^{1/2}\}$.

A simpler form to this Equation 90 can be derived if we ignore the temperature variation of physical properties. In this case Equation 88 integrates with $b_1 = b_2 = b_3 = b_4 = 0$, to give

$$T_s = T_0 \exp\left[\frac{-(\bar{W}\bar{C}_p + \Sigma UA)}{mC_p} \cdot t\right] + \frac{\bar{W}\bar{C}_p T_i + \Sigma UAT_a + I(E_T - \Delta H_r/nF)}{\bar{W}\bar{C}_p + \Sigma UA} \times \left[1 - \exp\left(\frac{-(\bar{W}\bar{C}_p + \Sigma UA)}{mC_p} \cdot t\right)\right] \quad (91)$$

This is a convenient expression for estimating the dynamic thermal characteristics of a CSTR. With assumptions of adiabatic operation and/or small heats of reaction, leads to the trivial equation.

$$T_s = T_p \exp\left(-\frac{\bar{W}t}{m}\right) + \left(\frac{T_i + IE_T}{WC_p}\right) \times \left[1 - \exp\left(\frac{-\bar{W}t}{m}\right)\right] \quad (92)$$

Equations 91 and 92, typically for electrosynthesis

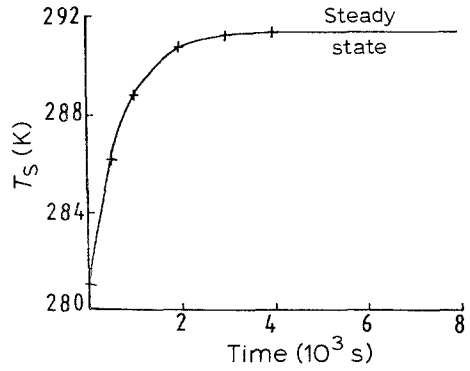

Fig. 18. Dynamic thermal response of a continuous stirred tank reactor. Conditions: $m = 20\,\text{kg}$; $n = 2$, $\Delta H_r = 30\,\text{kJ mol}^{-1}$, $UA = 100\,\text{W k}^{-1}$; $v\rho = 4 \times 10^{-3}\,\text{kg s}^{-1}$; $C_p = 4.2\,\text{kJ kg}^{-1}\,\text{K}^{-1}$; $I = 310\,\text{A}$, $T_0 = 281\,\text{K}$, $T_a = 278\,\text{K}$, $E_T = 4.1\,\text{V}$.

reactions at high current densities, predict the not too unfamiliar asymptotic rise in operating temperature to a final steady state value from a near ambient temperature. This is shown typically in Fig. 18, for the conditions indicated, where it is seen that it takes a time approximately equal to or greater than the residence time of the reactor to approach the steady state.

4.1. *Two compartment reactors*

The use of a separator in an electrolytic reactor divides the unit into two well-mixed compartments in which individual thermal energy balances apply. These balances now must accommodate the interchange of heat between anolyte and catholyte across the separator. This is due primarily to two processes. Convective heat transfer, defined through an appropriate overall heat transfer coefficient for the separator, U_s. Bulk energy flow which depends on the type of separator being employed and the species being transferred.

If the bulk heat exchange between anolyte and catholyte is small and if the reactor is operated with similar conditions in catholyte and anolyte, then the heat exchange will be relatively small and the reactor can be considered as a single unit. From the point of view of the thermal stability of the separator this is the preferred conditions of operation. However, the requirement of a high reaction efficiency is likely to determine final operating temperatures. For example, the desired reaction(s) at the working electrode may necessitate the use of a lower temperature in that stream. It could prove costly to cool both anolyte and catholyte streams to identical temperatures.

The mathematical picture of the thermal requirements of the CSTR has exclusively assumed that only one electrochemical reaction takes place, apart from the counter electrode reaction. To introduce further reactions would in general require associated material balances to be solved with a more elaborate energy balance. For electrochemical reactions where we can control the reaction rates through the current I it is sufficient to solve the energy balance independently. However, when homogeneous reaction(s) occur which exhibit a significant rate dependence on temperature, the material balance(s) and energy balance must be solved simultaneously. The energy balance will now include both Joule heat terms and heats of reaction of processes occurring at the electrode and in bulk solution.

4.2. *Thermal energy analysis for electrochemical reactors with homogeneous reaction*

Consider the following reactions in a continuous stirred tank electrochemical reactor.

$$\begin{aligned} O + 2e &\xrightarrow{i_1} A \\ A + B &\xrightarrow{k_1} P + O \end{aligned} \tag{93}$$

The reactor feed consists of a stream of $O + B$. The product $P(+B)$ is separated from the reactor outlet stream and unconverted A, plus regenerated O, are recycled.

This reaction is typical of the use of a redox mediator to carry out synthesis reactions where species A may be a metallic ions, halogen, etc.

The heat balance for this system is

$$I\left(E_T - \frac{\Delta H_{r1}}{nF}\right) - v\Delta H_{r2} X_B C_{B0} = \bar{W} C_p (T_s - T_i) + \sum UA(T_s - T_a) \tag{94}$$

where the second term on the left hand side represents heat generated by homogeneous reaction through the conversion X_B.

This expression is rearranged to give

$$X_B = \left[(T_s - T_i) + \frac{\sum UA}{v\rho C_p}(T_s - T_a)\right] \times \left(\frac{\rho C_p}{-\Delta H_{r2} C_{B0}}\right) - \left[\frac{1}{v\rho C_p}\left(E_T - \frac{\Delta H_{r1}}{nF}\right)\right] \times \left(\frac{\rho C_p}{-\Delta H_{r2} C_{B0}}\right) \tag{95}$$

For a first order homogeneous reaction the conversion is given by

$$X_B = \frac{k_1 \tau}{1 + k_1 \tau} \tag{96}$$

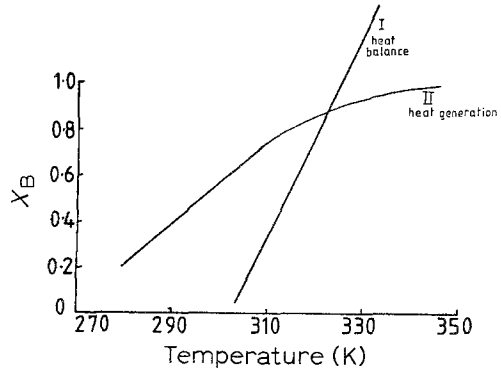

Fig. 19. Graphical solution to steady state operating temperature of coupled electrochemical and chemical reaction.

Equations 95 and 96 are functions of temperature and must be solved simultaneously. This can conveniently be done by a graphical construction, which is illustrated in Fig. 19.

5. Conclusions

This paper has attempted to bring together a number of important aspects of electrochemical reactor design based on the simple concept of a well mixed region with continuous flow in and out. The model of this system, the CSTR, is applicable to a large number of electrochemical processes and is widely adopted. Even when flow conditions depart from this ideal, the model can still be utilized through the concept of the tanks in series model of non-ideal flow. This application sees the power of the model in terms of ease of solution compared to other reactor models. Furthermore, this concept can be extended to model the behaviour of most types of reactor, ideal or not. Overall, therefore, the CSTR can be seen as the general purpose model in electrochemical reactor design.

References

[1] C. Y. Wen and L. T. Fan, 'Models for Flow Systems and Chemical Reactors', Marcel Dekker, NY (1975).
[2] K. R. Westerterp, W. P. M. van Swaajj and A. A. C. M. Beenackers, 'Chemical Reactor Design and Operation', J. Wiley & Sons, NY (1984).
[3] M. M. Jaksic, *Electrochim. Acta* **21** (1976) 1127.
[4] L. Weise, M. Giron, G. Valentin and A. Storck, 'Electrochemical Engineering' IChemE Symposium Series no. 98 (1986) p. 49.
[5] R. C. Alkire and J. D. Lisius, *J. Electrochem. Soc.* **132** (1985) 1879.
[6] R. H. H. P. Jaeger, L. J. J. Janssen, J. G. Wijen and E. Barendrecht, *J. Appl. Electrochem.* **13** (1983) 637.
[7] F. Goodridge, S. Harrison and R. E. Plimley, *J. Electroanal. Chem.* (1986).
[8] G. Kreysa and C. Woekcken, *Chemical Engng Sci.* **41** (1986) 307.
[9] G. P. Sakellaropoulos, *AIChEJ* **25** (1979) 781.
[10] E. Vieil, *Electrochim. Acta* **31** (1986) 263.
[11] D. J. Pickett, 'Electrochemical Reactor Design', Elsevier, Barking, Essex, 2nd ed. (1979).
[12] T. Z. Fahidy, 'Principles of Electrochemical Reactor Analysis', Elsevier, Barking, Essex (1985).
[13] J. M. Eldridge and E. L. Piret, *Chem. Eng. Progr.* **46** (1980) 290 Amsterdam.
[14] A. N. Haines, PhD Thesis, Teeside Polytechnic (1988).